International Journal of Environmental Science and Technology
https://doi.org/10.1007/s13762-020-02706-z

ORIGINAL PAPER

Association of geomorphic features with groundwater quality and freshwater availability in coastal regions

P. Prusty[1] · S. H. Farooq[1] · D. Swain[1] · D. Chandrasekharam[2]

Received: 21 November 2019 / Revised: 20 February 2020 / Accepted: 6 March 2020

Abstract
Seawater intrusion into coastal aquifers is a global problem as it limits the freshwater availability in coastal regions. A study has been conducted with the aims to identify the processes controlling seawater/freshwater distribution and demarcate potential freshwater zones in an aquifer along the coast of Bay of Bengal. Sixty-eight groundwater samples were collected from 900 sq. km spread along the coast and were analyzed for various physicochemical parameters. Most of the samples show brackish to saline characteristics. The anionic ratio indicates that 65% of groundwater samples are slightly to moderately affected by seawater, while 25% are severely affected. Seawater–freshwater mixing and freshening have been identified as the dominant processes in controlling the groundwater chemistry. Seawater has been traced in 88% of collected samples, and it is found that only 1% mixing of the seawater makes the groundwater unsuitable for drinking purposes. The fraction of seawater in individual samples has been calculated using chloride as a tracer. Thematic maps of seawater tracers have indicated that groundwater with higher salinity is located in the inland areas, whereas patches of fresh groundwater are found near the coast. With the help of satellite imageries, it has been found that the freshwater patches are typically located on paleochannels and sand dunes, which act as local reservoirs to retain freshwater in the seawater affected region. Such geomorphic features are common in coastal environments. Their identification and subsequent utilization as freshwater sources can be of vital importance to deal with freshwater scarcity in the coastal regions across the globe.

Keywords Coastal aquifer · Coastal water quality · Freshwater–seawater mixing · Saltwater intrusion

Introduction

Coastal regions are some of the world's most densely populated regions. The average population density in these regions is about 80 persons per km^2, which is twice the average population density of the world, thus enhancing the water demand in coastal areas (Kantamaneni et al. 2017). Consequently, to meet the ever-increasing water demand in these areas, groundwater resources are exploited indiscriminately (Re and Misstear 2017). Excessive groundwater pumping disturbs the hydrodynamic equilibrium and causes the reversal of hydraulic gradient near the coast, which in turn results in seawater intrusion into the inland areas of the aquifer (Abd-Elhamid et al. 2019). The inland migration of seawater in coastal aquifers is controlled by several factors such as hydraulic gradient, nature of geological formation (aquifer lithology), rate of groundwater recharge and withdrawal (Batayneh and Al-Taani 2016). Studies have further shown that geomorphology of the area and tidal activity also play significant roles in controlling the salinity of coastal groundwater (Aris et al. 2007; Hoque et al. 2016). In a few cases, it is found that the presence of paleo-seawater and salt pan may also increase the groundwater salinity and make them unusable (Nair et al. 2016). In structurally deformed coastal areas, the presence of deep-seated fault and lineament acts as potential pathways for the seawater to intrude the coastal aquifer much deeper into the land and mix with the fresh groundwater (Dhakate et al. 2016). Dissolution of evaporites, infiltration from irrigation

Editorial responsibility: M. Abbaspour.

✉ S. H. Farooq
hilalfarooq@iitbbs.ac.in

[1] School of Earth, Ocean, and Climate Sciences, Indian Institute of Technology Bhubaneswar, Argul, Khurda, Odisha, India

[2] Department of Civil Engineering, Indian Institute of Technology Hyderabad, Kandi, Sangareddy, Telangana, India

Published online: 13 March 2020

return, and geothermal and anthropogenic activities are the other causes of salinization of coastal groundwater resources (Sola et al. 2013; Mirzavand et al. 2020).

Freshwater scarcity in the coastal region is one of the fast-emerging problems, which severely hampers the living standards of coastal populations (Hussain et al. 2015). It has been reported that saline groundwater is being used for agricultural and industrial purposes in many coastal regions. The use of saline water not only reduces agricultural productivity but also affects the industrial growth of the region (Gopalakrishnan et al. 2019). Long-term ingestion of saline groundwater has many adverse health effects. In a few extremely susceptible coastal regions of Southeast Asia (India, Bangladesh, and Vietnam), a large population is forced to meet their daily water demand from the saline groundwater resources existing in the area. It is estimated that more than 7 million individuals living in these regions are suffering from hypertension and high blood pressure due to the direct ingestion of saline groundwater (Hoque et al. 2016). Additionally, the aquatic biota also gets severely affected by salinization of the surrounding ecosystem. Studies have well demonstrated the damaging effects of highly saline water on seeds of aquatic plants and eggs of microinvertebrates (Nielsen et al. 2003). Further, the deposition of salts on wetlands inhibits the nutrient distribution in plants and leads to leaf burn, defoliation, and their mortality (Herbert et al. 2015).

A significant number of studies have been conducted globally to understand the effect of seawater on groundwater quality in coastal aquifers (Michael et al. 2013; Cary et al. 2015; Nair et al. 2016; Zhang 2019; Mirzavand et al. 2020). Ten out of 12 European nations, including the coastline of Mediterranean (in Italy, Spain, and Turkey), are facing the problem of increased salinity (Scheidleger et al. 2004; Daliakopoulos et al. 2016). The contamination of coastal groundwater by seawater has also been observed in the USA, Mexico, and Canada, where it has caused the closure of many wells (Barlow and Reichard 2010). The coastal population in Africa, surrounded by five major saline water bodies, has the highest threat of salinization due to sea level rise, coastal flooding, and seawater intrusion (Pink 2018). In the case of Australia, the coastal wetlands are severely affected by salinization that has impacted indigenous flora and fauna (Saintilan et al. 2018). The salinization of water has been reported as a major problem in many coastal regions in Asia, for example in Bengkalis Island, Indonesia (Putra et al. 2019), central coastal plains of Japan (Yamanaka et al. 2014), coastal regions of China (Shi and Jimmy 2014), Ho Chi Minh City of Vietnam (Ngo et al. 2015), coastal areas of Jazan, Saudi Arabia (Abdalla 2016), southwestern coast of Bangladesh (Rakib et al. 2020), and along the coastal stretch of India (Manivannan and Elango 2019). Almost all coastal districts of India are facing either the seawater intrusion or issues related to higher soil salinity (Fig. 1; MoEF & CC 2016). The Indian states, namely Gujarat, Andhra Pradesh, Tamil Nadu, and Odisha, are some of the most severely affected regions facing the problem of groundwater salinization (Central Water Commission 2017). An area of $\approx$5000 km^2 spreading over six districts in the state of Odisha and inhibiting about 11.6 million people (27.7% of the total population of the state) is under direct salinity hazards (Central Water Commission 2017). An earlier study conducted along the coastal regions of Puri district, Odisha demonstrates that around 50% of the groundwater samples are saline in nature, and their chemical characteristics do not show significant seasonal variability (Prusty et al. 2018). Based on multivariate statistical analysis, it has been reported that the deterioration of groundwater quality in the area is caused by the mixing of seawater with the groundwater (Mohapatra et al. 2011). These studies, however, lack the quantification of seawater–freshwater mixing and identification of possible potential freshwater regions in a seawater affected area. Such aspects are essential for a detailed understanding of processes that control the groundwater chemistry and may help in the efficient management of the coastal water resources.

In the present study, an attempt has been made to fill the gaps in scientific knowledge. The study aims to (1) link the processes that control the groundwater salinity in the coastal aquifer with the degree of seawater–freshwater mixing at individual well level, and (2) locate the potential freshwater regions within the seawater affected area. For this purpose, a unique multi-dimensional approach integrating hydrochemical tools with remote sensing and geographical information system (GIS) tools have been adopted to understand the seawater and freshwater distribution in the study area (i.e., Puri district of Odisha, India). Further, satellite imageries of the area were used to identify the geomorphic features and establish their possible association with the distribution of freshwater. The outcome of the present study will contribute to a more efficient management of coastal groundwater resources, which in turn will have a positive impact on the health and livelihood of the coastal population.

Materials and methods

Study area

The coastal tract of the state of Odisha presents a flat or gently undulating terrain with a NE–SW trend. Puri, a major populated coastal district of Odisha, is situated along the Bay of Bengal shore. Geographically, it extends between 19° 40′–20° 10′ N latitudes and 85° 25′–86° 25′ E longitudes with the Chilika lake in the southwest and the Devi river in the northeast. The district spreads over

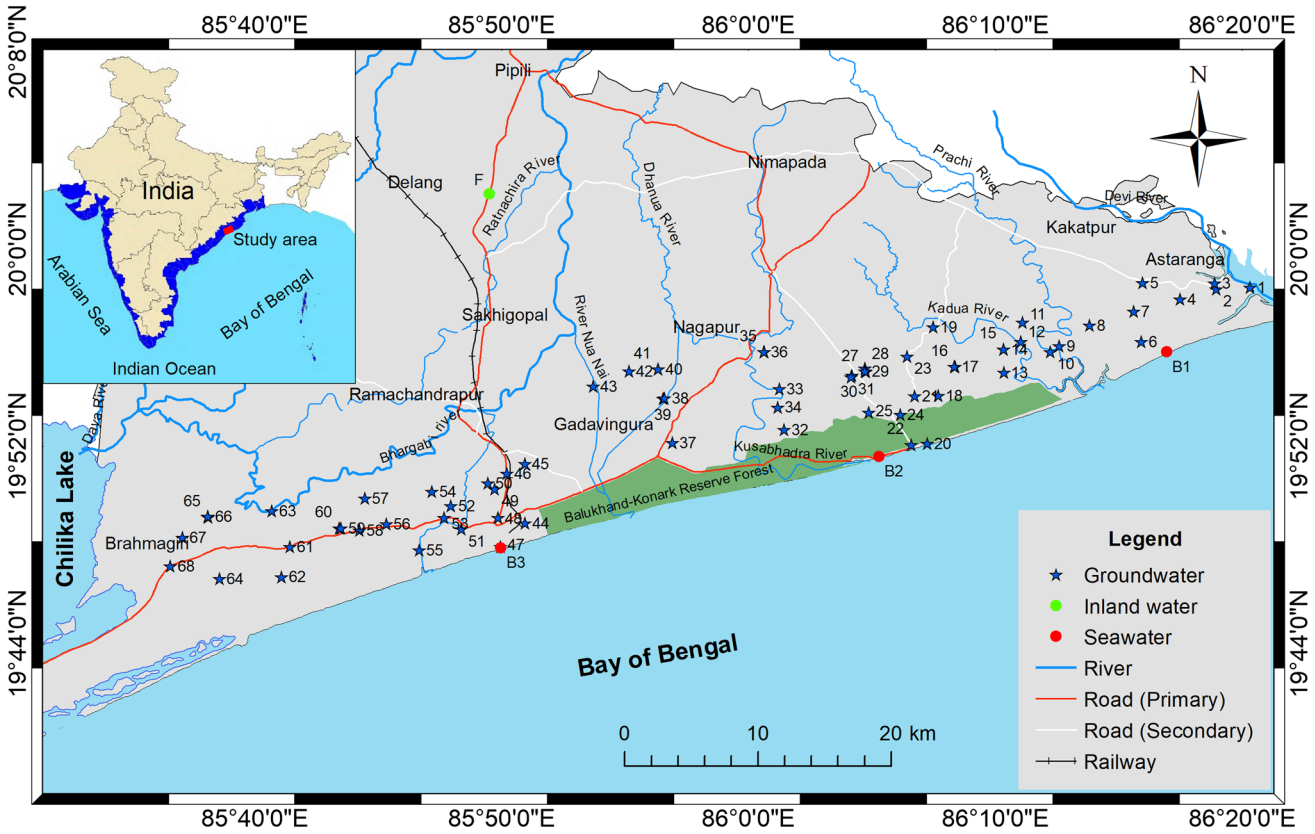

Fig. 1 Water sampling locations in the study area (Coastal regions of India affected by groundwater or soil salinity hazards are highlighted in blue colored; MoEF & CC 2016)

nearly 3479 km^2 areas with a population density of 488 individuals per km^2, and the population is increasing at a rate of 13% over the past 10 years (Census of India 2011). In recent times, the withdrawal of groundwater has increased by several folds with the opening of several industries in this region. The district has rock formations of varying age from Archean to Recent with the major parts being covered by the Tertiary and Quaternary formations and exposure of Archean rocks in the hilly regions (Central Ground Water Board 2013). The Archean rocks, including granite, gneisses, charnockites, and khondalites, act as basement rocks, which are covered by the unconsolidated alluvial deposits of Tertiary and Quaternary age. These alluvial cover sediments are the main water-bearing formations of the area, where the shallow groundwater is present under phreatic conditions and the deeper groundwater under semiconfined condition. The district is in the Mahanadi river basin that receives an average annual rainfall of nearly 1450 mm from the southwest monsoon during June–October (Patra et al. 2012). The region usually experiences a warm and humid climate.

Sampling and analytical methods

Groundwater samples collected from 68 tube wells during the post-monsoon season in 2016 were considered in the present study. These tube wells have an average depth of 13–15 m and are distributed from the shoreline up to a distance of 10 km in Puri district. The water from these tube wells is mainly used for drinking purposes. In addition to these samples, one furthermost inland groundwater (not affected by the seawater) and three seawater samples from the Bay of Bengal have also been collected for the purpose to estimate the mixing of seawater with the fresh groundwater. Each sampling location was geo-referenced with the help of a hand-held Global Positioning System (GPS; Trimble Juno S-3 model), and the sample location map is shown in Fig. 1. The stagnant water in the well casing was purged prior to sample collection by pumping the tube wells for a period of 3–5 min. At each location, two water samples (each of 250 ml) were collected in pre-cleaned polyethylene bottles: (1) filtered samples (0.45-µm polycarbonate membrane filter) with no addition of acid; and (2) filtered and acidified (with the addition of ultrapure HNO_3) samples. A

pre-calibrated portable multi-parameter system (Orion Star A329, Thermo Fisher Scientific) was used for in situ measurement of pH and electrical conductivity (EC) in the water samples. Total dissolved solids (TDS) were calculated from the expression involving the EC values: TDS (mg/l) = EC (µS/cm) × 0.64 (Lloyd and Heathcote 1985). Subsequently, the collected water samples were analyzed for major ion concentrations in the laboratory. The cations, including sodium (Na), potassium (K), calcium (Ca), and magnesium (Mg), were analyzed in the acidified samples and the anions, including chloride (Cl) and sulfate (SO_4), in the non-acidified samples by Ion Chromatography System (883 Basic IC Plus, Metrohm). Total alkalinity, consisting of carbonate (CO_3) and bicarbonate (HCO_3), was determined in the non-acidified samples by titrimetric analysis (848 Titrino plus, Metrohm; Rice et al. 2012). A synoptic view of the methods applied in the present study is presented in the form of a flowchart (Fig. 2).

Remote sensing and GIS analysis

Remote sensing and GIS techniques have been proved to be excellent tools and are being used extensively in hydrological studies. In the present study, they have been integrated with hydrochemical tools to understand the groundwater potential of coastal aquifer. Thematic maps of hydrochemical parameters and seawater tracers were prepared to observe the spatial distribution of seawater–freshwater in the study area. For this purpose, a widely used interpolation technique, inverse distance weighted (IDW) method has been utilized (Kanagaraj et al. 2018). This interpolation method considers more influence of the neighboring points in comparison to the distal points; thus, this can be more effectively used in the coastal area, where the data varies unevenly (Prasanth et al. 2012). Natural breaks classification method, which is the best method for optimization of variation within and between groups, was adopted for the classification of data sets in the thematic maps to understand the spatial distribution of seawater–freshwater in the area (Sun et al. 2017). Satellite imageries of the area were utilized to find out the relationship of seawater–freshwater distribution with the coastal geomorphic features. Digital elevation model (DEM; 30 m resolution) from the Shuttle Radar Topography Mission (SRTM), Thermal infrared false-color composite (TIR-FCC) image (Landsat 8, February-2017), and Enhanced Thematic Mapper Plus (ETM +) Pan Mosaic image (Landsat 7, November-1999) were utilized to identify the geomorphic features existing in the study area (Nandini et al. 2013;

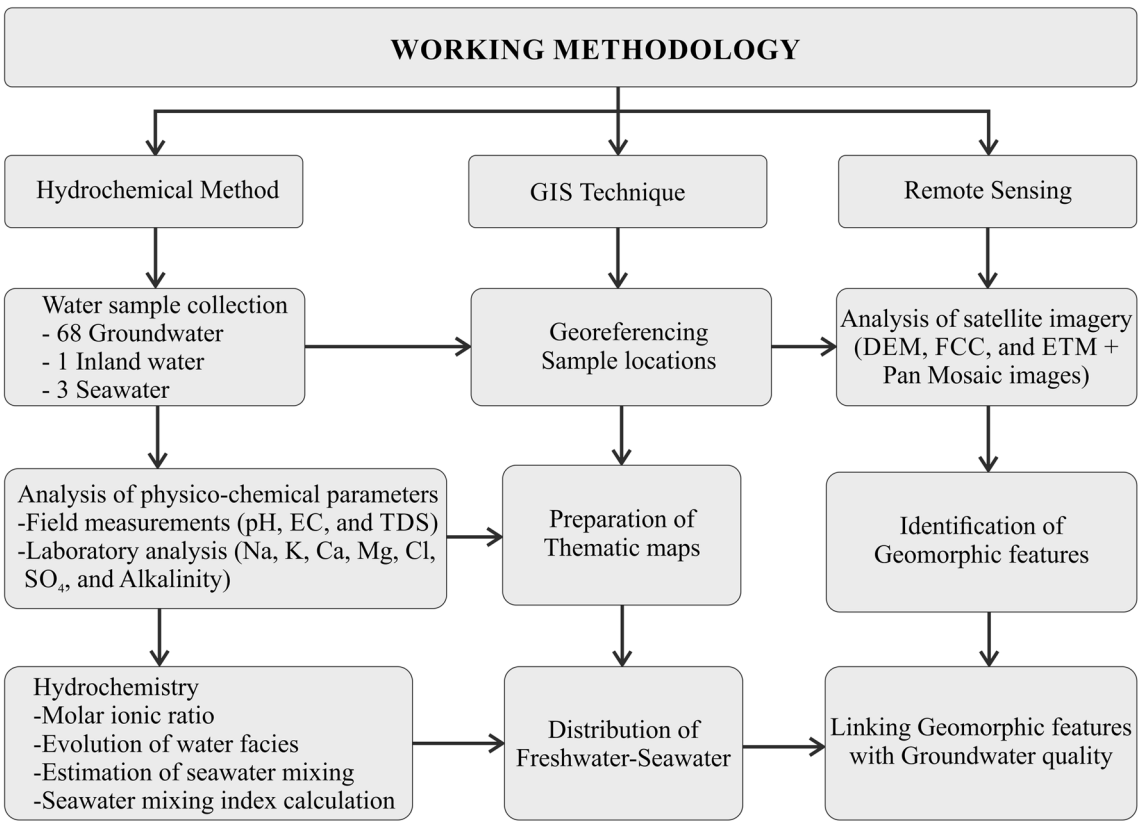

Fig. 2 Flowchart of the methods adopted in the study

Table 1 Statistical summary of physicochemical parameters measured in the collected groundwater samples ($n=68$) in comparison with WHO standards

Parameters	Collected groundwater samples			WHO permissible limit for drinking water	Samples (%) beyond the WHO limit
	Mean	Minimum	Maximum		
pH	7.0	5.2	8.2	6.5–8.5	10.3
EC	3395	94.1	21,180	1500	55.9
TDS	2173	60.2	13,555	1000	55.9
Alkalinity	235.1	6.9	703.0	600	1.47
Cl	866.0	6.1	7139	600	44.1
SO_4	118.8	0.1	1433	250	8.82
Na	521.0	6.3	3921	200	57.4
K	35.4	1.1	162.1	–	–
Ca	93.2	0.3	1069	200	10.3
Mg	72.5	1.1	796.7	150	7.35

pH in numerical value, EC in µs/cm, and all others in mg/l

Afrasinei et al. 2018). For better appearance, the images were enhanced by the histogram stretching technique. ArcMap (10.2) has been used for the preparation of thematic maps and satellite imagery analysis.

Results and discussion

Hydrochemistry of coastal groundwater

The collected groundwater samples are slightly acidic to mildly alkaline in nature, with a pH range of 5.2–8.2 and an average pH of 7 (Table 1). Seven out of 68 samples (10%) have pH values less than the World Health Organization (WHO) permissible limit for drinking water (6.5–8.5). In these seven samples, the pH value varies from 5.2 to 6.4. The acidic nature of groundwater causes higher accumulation of toxic metals in the water that may lead to aesthetic issues like staining of laundry, sinks, drains, metallic or sour taste, etc. (Oram 2011). TDS content varies widely (60.2–13,555 mg/l) in the collected groundwater samples with its average value (2173 mg/l) exceeding the WHO permissible limit (1000 mg/l). Around 56% of samples are found to be unsuitable for drinking purposes due to their higher TDS contents (Table 1). The higher TDS values in coastal groundwater are generally attributed to the impact of seawater mixing that supplies higher concentrations of major ions to the groundwater (Mondal et al. 2010). Based on TDS content, groundwater can be categorized as freshwater, brackish water, saline water, and brine (Freeze and Cherry 1979). Around 44% of the collected water samples fall under freshwater type (< 1000 mg/l), while the remaining 56% of samples vary from brackish to saline water types (> 1000 mg/l) suggesting possible contamination from the seawater in the study area (Table 2). The detailed analytical data of individual samples is provided in "Appendix."

Table 2 Classification of groundwater based on TDS content (Freeze and Cherry 1979)

TDS (mg/l)	Water type	No of samples	Percentage
< 1000	Fresh	30	44.1
1000–10,000	Brackish	35	51.5
10,000–100,000	Saline	3	4.4
> 100,000	Brine	Nil	Nil

The major ion concentrations in the collected groundwater samples show a wide variation. The maximum variation among the cations is shown by Na (6.3–3921 mg/l) and the least variation by K (1.1–162.1 mg/l). Chloride (6.1–7139 mg/l) shows the highest ionic concentration as well as the highest variation in concentration among all the ions. The range of Ca, Mg, SO_4, and HCO_3 concentrations in the collected groundwater samples is 0.3–1069 mg/l, 1.1–796.7 mg/l, 0.1–1433 mg/l, and 6.9–703 mg/l, respectively. The dominance of Na and Cl ions with higher major ion concentrations in coastal groundwater indicates the interaction of seawater with the groundwater (Mohanty and Rao 2019). In addition to higher Na and Cl concentrations, other major ion concentrations are also found exceeding the WHO permissible limits for drinking water in a few of the collected groundwater samples (Table 1); thus, they are not suitable for drinking purposes. Studies have shown that under certain circumstances, higher salinity in groundwater can be due to excessive trace element concentrations (Deverel et al. 2011). It has been reported that the trace elements are present in very low concentrations in the groundwater of the area and do not show any significant relationship with the groundwater salinity (Prusty et al. 2018).

Groundwater salinity and controlling factors

Molar ionic ratios of different elements have been utilized as excellent geochemical indicators for understanding hydrological systems (Abdalla 2016). In a coastal hydrological system, HCO_3 and Cl represent freshwater and seawater, respectively (Sajil Kumar et al. 2014). In this study, Cl/HCO_3 molar ratio has been plotted against Cl concentrations to know the effect of salinization on groundwater (Najib et al. 2017). The Cl/HCO_3 ratio varies from 0.1 to 157 in the collected groundwater samples. The highest ionic ratio of 374 is obtained for the collected seawater sample, and the inland groundwater sample has a ratio of 0.36. In the ionic ratio plot, the inland groundwater and seawater samples fall on the "not affected" and "strongly affected" regions, respectively (Fig. 3). Among the collected groundwater samples, only seven groundwater samples (10%) have Cl/HCO_3 ratios less than 0.5, which indicates that these samples are not affected by salinization (Fig. 3). In about 25% of the samples, salinization has a strong influence in modulating the groundwater chemistry, which is reflected in the form of their higher Cl/HCO_3 ratios (> 6.6). The remaining 65% of the samples that lie in between (i.e., within not affected to strongly affected) indicate varying degree of mixing of seawater with fresh groundwater.

Hydrochemical facies evolution (HFE) diagram is widely used to understand the evolution of groundwater in the coastal aquifer (Mirzavand et al. 2020). The HFE diagram requires the chemical composition of a seawater sample and a freshwater sample to be used as seawater and freshwater end-members, respectively (Giménez-Forcada 2019). The average chemical composition of the three seawater samples collected from the Bay of Bengal has been considered as the seawater end-member, while the composition of freshwater end-member (highest Ca and HCO_3 concentrations) has been derived from the collected groundwater samples for the plotting of HFE diagram. Distribution of samples in the HFE diagram shows that groundwater in the study area is characterized mainly by Na–Cl (72%) and Na–HCO_3 (7%) water types. The evolution of groundwater facies can be explained by freshening and intrusion processes, assisted by direct ion-exchange, reverse ion-exchange, and seawater–freshwater binary mixing processes (Fig. 4; Giménez-Forcada 2010). The samples that fall above and the left of the conservative mixing line indicate the freshening phase, while the samples falling below and the right of the mixing line indicate the intrusion phase. With the initiation of the freshening phase, the Na–Cl water changes to Na–mixCl, followed by Na–mixHCO_3 and Na–HCO_3 (i.e., following the evolution path 4–3–2–1 fields of the diagram; Fig. 4). During the freshening phase, direct ion-exchange process takes place through which the groundwater gains Na from the aquifer with the exchange of Ca from the water and develops Na–HCO_3 water facies in the groundwater (Sola et al. 2013). At the end of the freshening phase, the Na–HCO_3 water progresses toward the recharging water (Ca–HCO_3) through MixNa–HCO_3 and MixCa–HCO_3 (evolution path: 1–5–9–13; Fig. 4). In the intrusion phase, the recharging

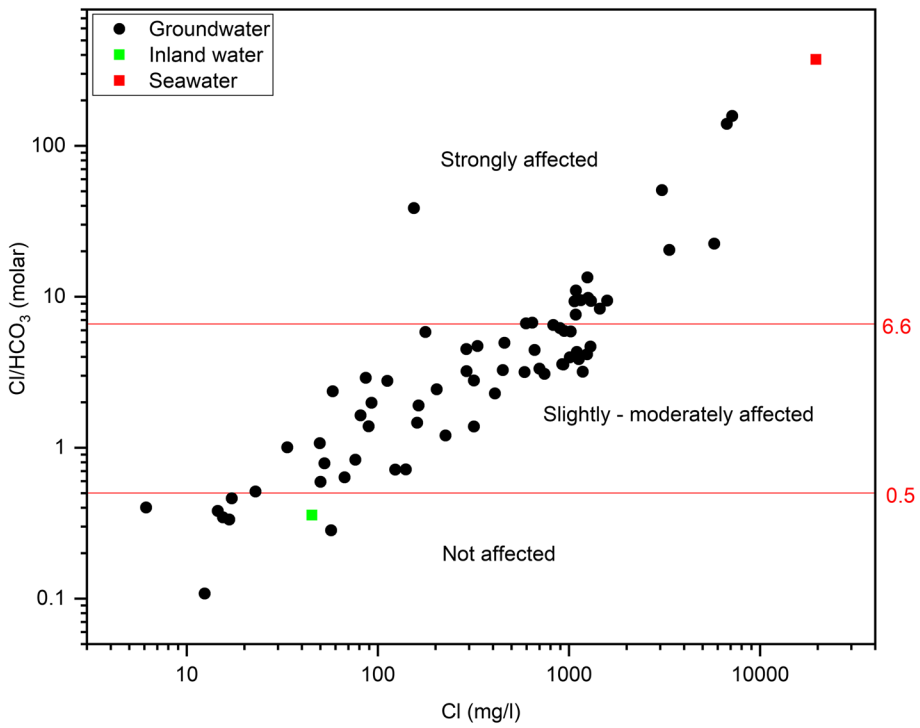

Fig. 3 Bivariate plot of Cl versus Cl/HCO_3 depicting the effect of salinization on groundwater quality

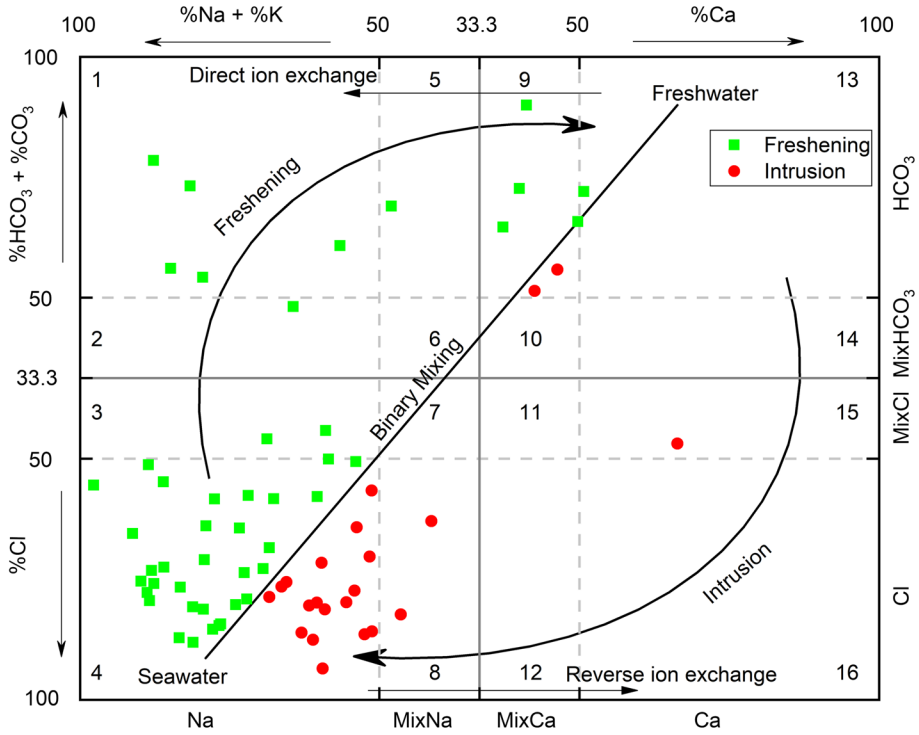

Fig. 4 Evolution of groundwater facies in hydrochemical facies evolution diagram. 1: Na–HCO_3, 2: Na–MixHCO_3, 3: Na–MixCl, 4: Na–Cl, 5: MixNa–HCO_3, 6: MixNa–MixHCO_3, 7: MixNa–MixCl, 8: MixNa–Cl, 9: MixCa–HCO_3, 10: MixCa–MixHCO_3, 11: MixCa–MixCl, 12: MixCa–Cl, 13: Ca–HCO_3, 14: Ca–MixHCO_3, 15: Ca–MixCl, 16: Ca–Cl

water gets salinized with the mixing of Na–Cl water. The reverse ion-exchange process enriches Ca in the groundwater with the development of Ca–Cl water (vice versa of direct ion-exchange process) during the intrusion phase. Only one sample falls in field 15, which indicates the initial phase of intrusion (evolution path: 13–14–15–16; Fig. 4). The samples in the intrusion phase are mostly in the final stage of intrusion, where the Ca–Cl water has changed to Na–Cl water (evolution path: 16–12–8–4; Fig. 4). However, the samples in the freshening or intrusion phases that fall on or very close to the mixing line are considered to be evolved dominantly by the simple binary mixing process between the freshwater and seawater end-members without a significant interference of the ion-exchange processes. Hence, the Na–Cl water in field 4 indicates their evolution either by the initial phase of freshening or by the last stage of intrusion or by simple binary mixing.

The intrusion and freshening phases can also be confirmed by comparing the observed ionic concentrations with the theoretical ionic concentrations for a particular water sample. The theoretical concentration of an ion '*I*' (I_t) can be calculated from the conservative mixing of freshwater and seawater end-members using the Expression-1, where F_{sea} represents the fraction of seawater in the sample; I_{sea} and I_{fresh} represent the concentrations of the ion '*I*' in seawater and freshwater, respectively (Appelo and Postma 2005). Chloride behaves as a conservative ion; thus, its concentration can be used as a tracer to calculate the fraction of seawater in each groundwater sample (Sola et al. 2013).

The fraction of seawater in the groundwater samples has been calculated from the Cl concentrations of the samples (Cl_{sample}) with respect to a freshwater (Cl_{fresh}) and a seawater (Cl_{sea}) end-member using the Expression-2 (Appelo and Postma 2005). For this purpose, the collected seawater was considered as the seawater end-member and the furthermost inland freshwater sample as the freshwater end-member. The deviation in ionic concentration (I_{change}) is calculated as the difference between the observed (I_{sample}) and theoretical concentrations of the ion '*I*' (Expression-3). For all these calculations, the concentrations of ions are in milliequivalent per liter (Meq/l).

$$I_t = F_{sea} \times I_{sea} + \left(1 - F_{sea}\right) \times I_{fresh}, \tag{1}$$

$$F_{sea} = \left(Cl_{sample} - Cl_{fresh}\right) / \left(Cl_{sea} - Cl_{fresh}\right), \tag{2}$$

$$I_{change} = I_{sample} - I_t. \tag{3}$$

In order to understand the effects of seawater mixing on groundwater chemistry, the sample locations are rearranged based on three parameters, i.e., the fraction of seawater in the samples, the distribution of samples in the HFE diagram, and the deviation between the observed and theoretical concentrations. A positive fraction of seawater in 88% of samples suggests the dominance of the seawater–freshwater mixing process in the area (Fig. 5a). In the remaining 12% of samples, the seawater fraction has a negative value

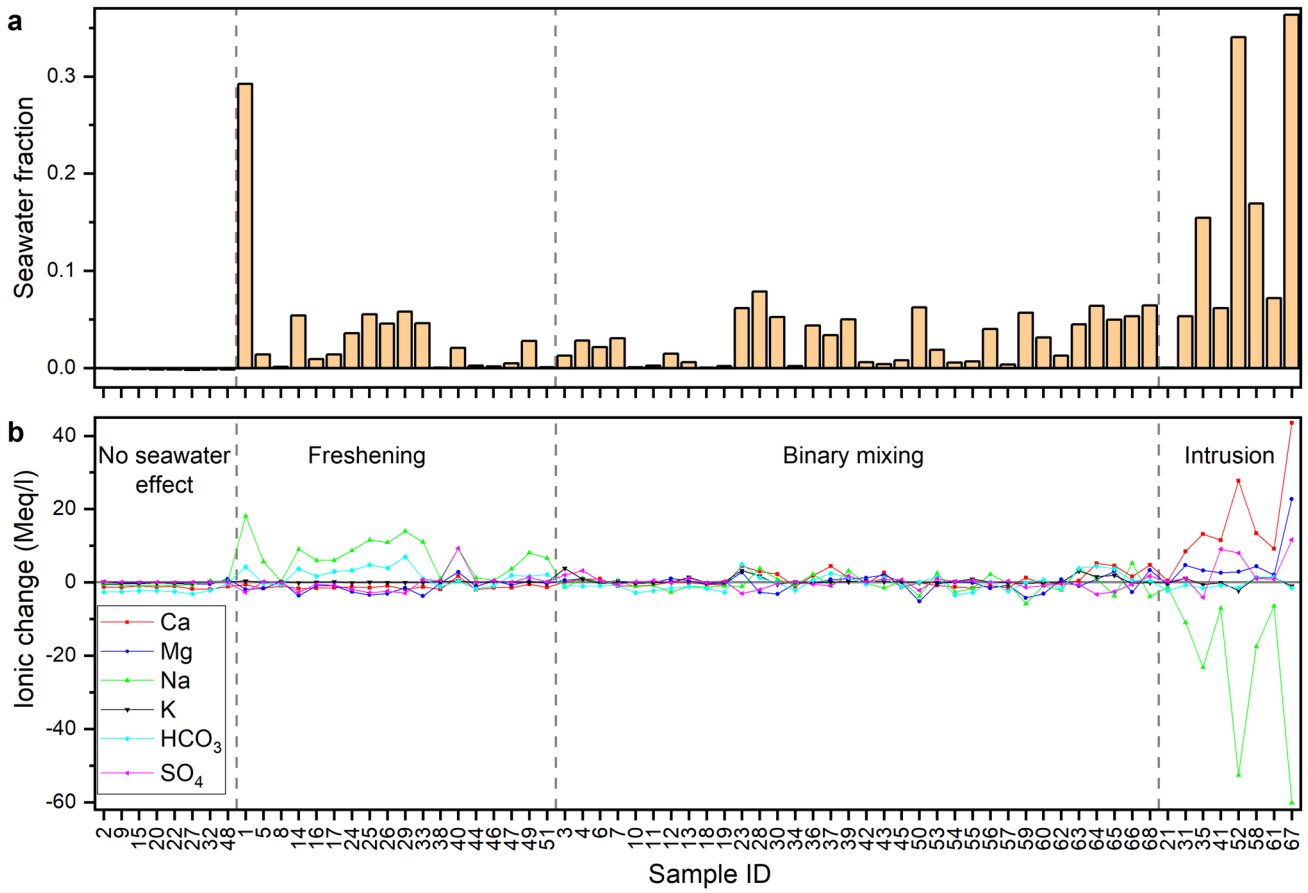

Fig. 5 Dominant processes controlling groundwater salinity. **a** Fraction of seawater in individual samples and **b** deviation of measured ionic concentrations from the theoretical concentrations

indicating that the seawater mixing process does not modulate the water chemistry in these samples. Significant mixing has been observed in 7% of samples where the seawater percentage is more than 10% ($F_{sea} > 0.1$). It has been found that around 1% mixing of seawater with the fresh groundwater is sufficient to increase the TDS values higher than the WHO permissible limit (1000 mg/l) and make them unusable for drinking purposes. The ionic changes between the observed and theoretical concentrations for Na, K, Ca, Mg, HCO_3, and SO_4 at each sampling location are presented in Fig. 5b. In 50% of samples, the deviation of observed ionic concentrations from the theoretical concentrations is negligible, and these samples are falling close to the mixing line in the HFE diagram. Thus, it is confirmed that these samples have been evolved by the simple binary mixing process without any involvement of the ion-exchange processes (Fig. 5b). The presence of excessive Na in 26% of samples than the seawater–freshwater mixture indicates that the freshening process aided by the direct ion-exchange process plays an important role in controlling the groundwater chemistry in these samples. The same is reflected in the form of placement of these samples in the freshening phase and away from the mixing line in the HFE diagram. On the other hand, the remaining 12% of samples show a positive ionic change for Ca (Fig. 5b). These samples are falling in the intrusion phase and away from the mixing line in the HFE diagram, thus confirms their evolution through the intrusion process. Other processes like $CaCO_3$ dissolution or precipitation and SO_4 reduction are not significant in the area since the HCO_3 and SO_4 concentrations in the groundwater do not show much deviation from the theoretical values (Fig. 5b; Giménez-Forcada 2019).

Seawater mixing index (SMI)

SMI was calculated to estimate the degree of seawater mixing in the collected groundwater samples. The calculation of SMI involves the concentrations of Na, Mg, Cl, and SO_4 in water samples and their relative proportions in the seawater. The SMI for each groundwater sample can be calculated using the Expressed-4, where *a*, *b*, *c*, and *d* are the relative proportions of Na, Mg, Cl, and SO_4 in the seawater, respectively; *C* is the measured concentration (mg/l) in the water samples; *T* is the regional threshold values for the respective

ions (Park et al. 2005). The regional threshold values are obtained from the inflection points on their cumulative probability curves (Sinclair 1974; Kanagaraj et al. 2018). The average ionic concentrations of the collected seawater samples have been used as the seawater composition for the calculation of the relative proportion of the ions.

$$\mathrm{SMI} = a \times \frac{C_{\mathrm{Na}}}{T_{\mathrm{Na}}} + b \times \frac{C_{\mathrm{Mg}}}{T_{\mathrm{Mg}}} + c \times \frac{C_{\mathrm{Cl}}}{T_{\mathrm{Cl}}} + d \times \frac{C_{\mathrm{SO_4}}}{T_{\mathrm{SO_4}}} \quad (4)$$

The method to estimate regional threshold value for Na, Mg, Cl, and SO_4 from their cumulative probability curves is shown in Fig. 6a. For each ion, two threshold values were obtained. The lower threshold values (Na: 349 mg/l, Mg: 21 mg/l, Cl: 644 mg/l, and SO_4: 16 mg/l) were considered for the calculation of SMI (Fig. 6a). The relative concentration proportions of the ions in the seawater were found as: $a = 0.33$, $b = 0.04$, $c = 0.54$, and $d = 0.07$. The SMI value varies from 0.02 to 16.4 in the groundwater samples. The samples having negative seawater fraction (≈ 0) have much

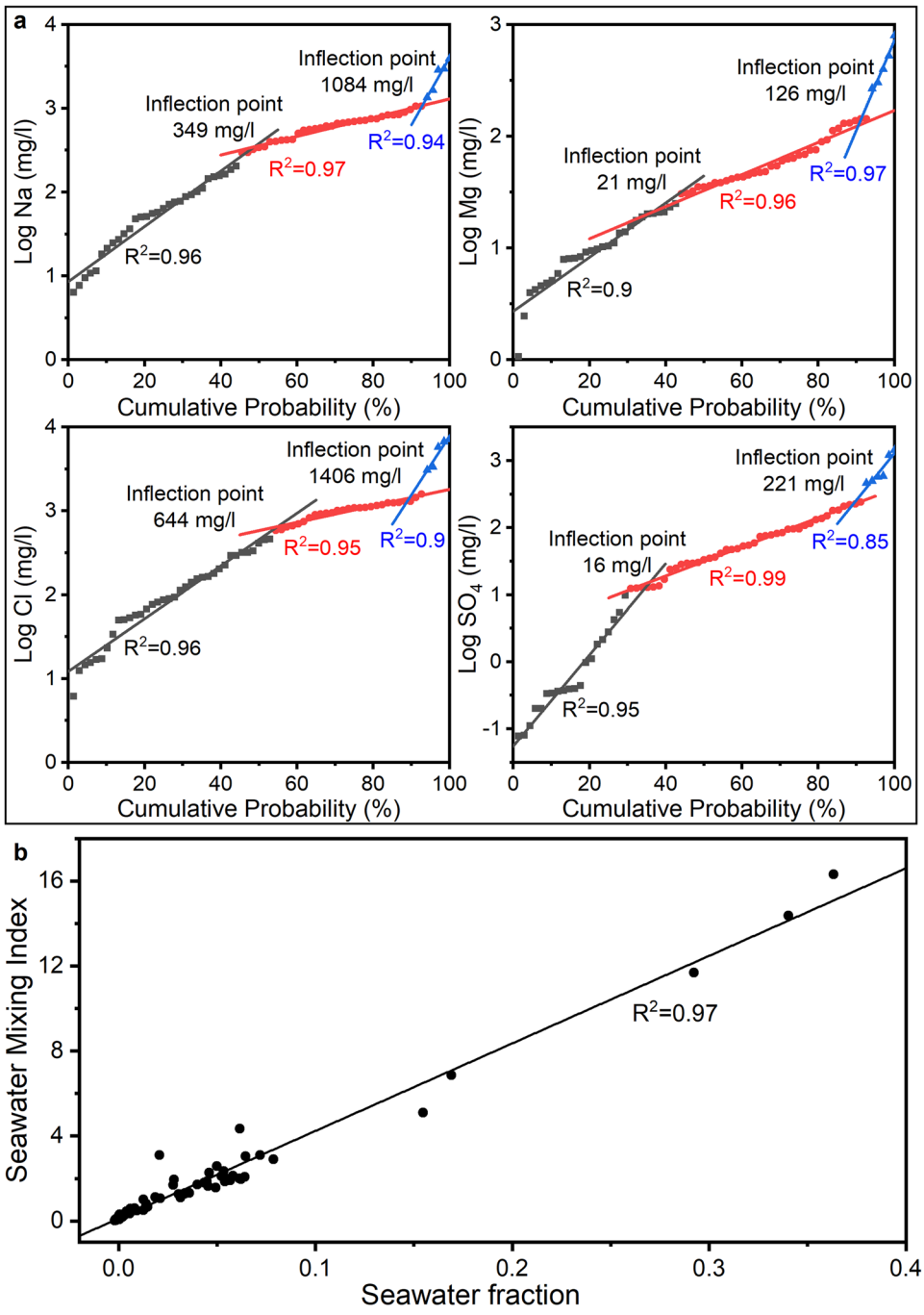

Fig. 6 **a** Estimation of regional threshold values of Na, Mg, Cl, and SO_4 from their cumulative probability curves; and **b** Relationship between seawater mixing index and seawater fraction

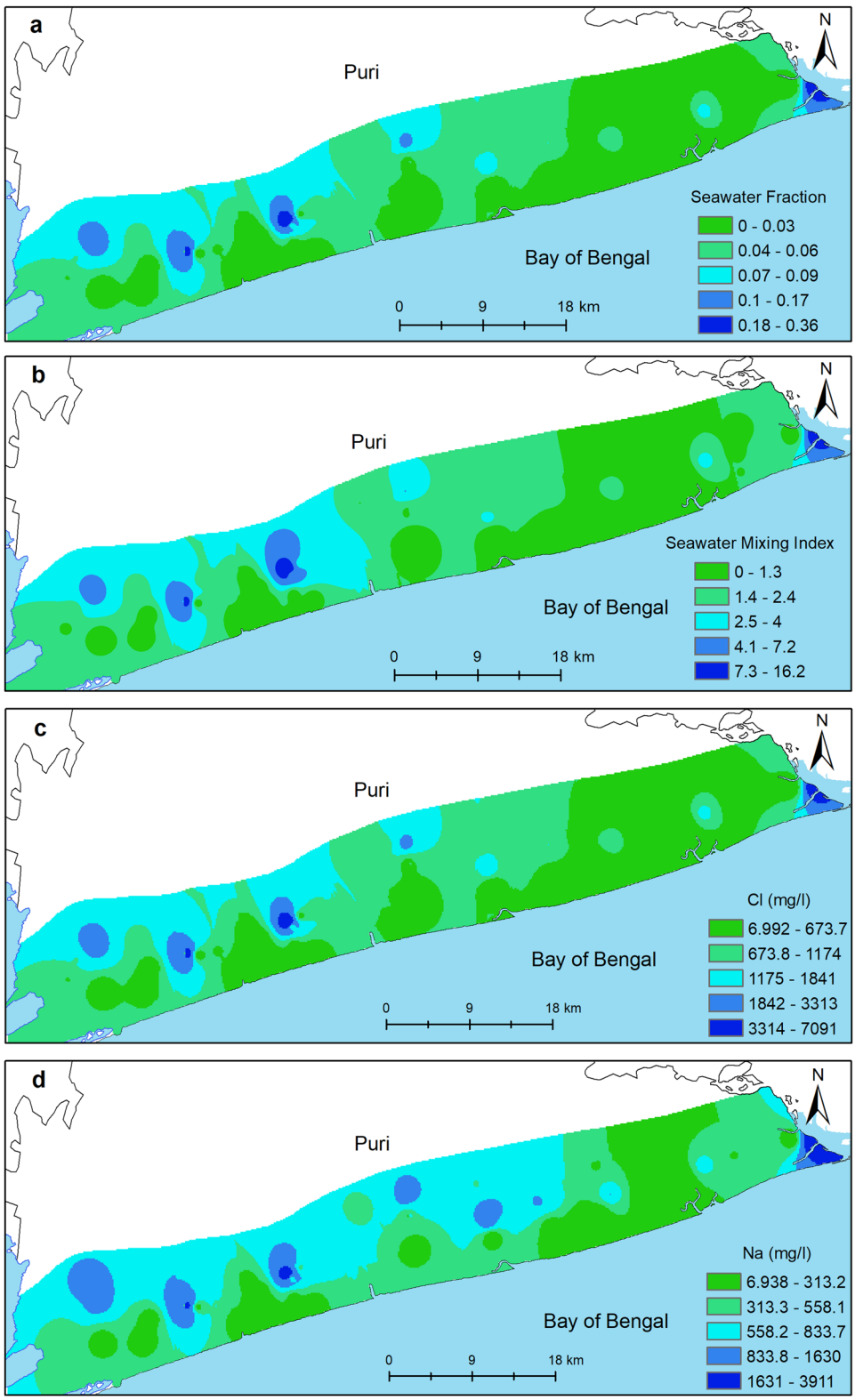

Fig. 7 Thematic maps showing the distribution of **a** seawater fraction, **b** seawater mixing index, **c** Cl, and **d** Na in the study area

lesser SMI values, while samples with positive seawater fraction have higher SMI values (Fig. 6b). SMI values more than 1 were found in 53% of samples, which gives a clear indication of seawater mixing in the area (Park et al. 2005). This is also observed from the strong relationship ($R^2 \sim 1$) between SMI and seawater fraction (Fig. 6b).

Locating potential fresh groundwater resources

Thematic maps have widely been utilized in hydrological studies for visualization of spatial variations in data sets (Ghasemlounia and Sedaghat Herfeh 2017; Solangi et al. 2019). In the present study, the fraction of seawater in groundwater samples, seawater mixing index values, and concentrations of Cl and Na have been used as seawater tracers, and their thematic maps were used to observe the spatial distribution of seawater–freshwater in the study area. The thematic maps of these parameters show similar distribution patterns in the study area (Fig. 7a–d). It is evident from the thematic maps that higher values of these parameters are located in the inland area and lower values close to the sea. This leads to an interesting finding that the groundwater located in the inland areas are more affected by the seawater, whereas patches of fresh groundwater are found close to the coast (Fig. 7a–d).

Geomorphic features play a significant role in controlling the subsurface seawater–freshwater distribution in coastal areas. The geomorphic features like sand dunes and buried paleochannels have higher permeability and can form excellent aquifer in coastal regions (Owen and Dahlin 2010; Nandini et al. 2013). The existence of sand dunes in the area has been cross-checked during field visits. In the present study, the DEM image of the area has been utilized to identify the sand dunes based on their sharp and higher elevation contrast near the coast (Fig. 8a). The present river channels were traced on the FCC image characterized by their spectral signature (Fig. 8b). Water bodies (blue), vegetation (green), and sands (pink) were identified on the ETM + Pan Mosaic image based on their color coding (Fig. 8c). Higher elevation from the DEM image and presence of sand bodies from the ETM + Pan Mosaic image of the area reconfirm the occurrence of the sand mound and dune systems near to the coast (Fig. 8a, c). The presence of sand dunes along the coast has also been reported by other studies (Central Ground Water Board 2014). Further, a comparison of drainage patterns from the recent FCC image (2017) with the past ETM + Pan Mosaic image (1999) reveals the existence of a network of paleochannels in the area (Fig. 8b, c). The spatial distribution of groundwater sample locations on these images indicated that most of the wells containing fresh groundwater (TDS < 1000 mg/l) occur either on the dunes or paleochannels existing along the coast. Studies have shown the existence of thin layers of clay in the unconfined sandy aquifers in the study region at shallow depths (Vijay et al. 2011; Mohanty and Rao 2019). These clayey layers not only restricts the downward movement of freshwater accumulated in paleochannels and sand dunes but also prevent the upward movement of the seawater. Thus, it limits the seawater–freshwater mixing locally and helps in the formation of perched aquifers. These findings are in-line with other studies conducted in various coastal regions of the globe (Schneider and Kruse 2003; Viso et al. 2010). Geophysical methods such as vertical electrical sounding (VES) and electrical resistivity tomography (ERT) have widely been applied for subsurface mapping in groundwater studies (Dhakate et al. 2016; Kanagaraj et al. 2018). A detailed geophysical survey of the coastal regions may provide precise information about the depth, extent, and geometry of the perched aquifers, which in turn will help in determining their groundwater potentials.

Conclusion

The study highlights that the groundwater samples in the study area are mostly of Na–Cl type, and 88% of the samples are affected by the seawater. The mixing calculations, involving seawater and freshwater as end-members, show that 1% mixing of the seawater is sufficient to raise the TDS values > 1000 mg/l in 56% of the groundwater samples and make them unsuitable for drinking purposes. The evolution of hydrochemical facies indicates that seawater–freshwater mixing (50%) and freshening due to ion-exchange process (26%) are the dominant processes in controlling the groundwater chemistry. Strikingly, the thematic maps of various seawater tracers reveal the occurrence of fresh groundwater pockets close to the shoreline and brackish-saline groundwater in the inland areas. The high-resolution DEM, ETM + Pan Mosaic, and FCC images establish that these freshwater pockets are located on commonly occurring coastal geomorphic features such as sand dunes and paleochannels. These geomorphic features act as perched aquifers and hold freshwater even in the seawater affected regions. Their identification and utilization may provide a sustainable solution to deal with the problem of freshwater scarcity in seawater affected coastal regions across the globe.

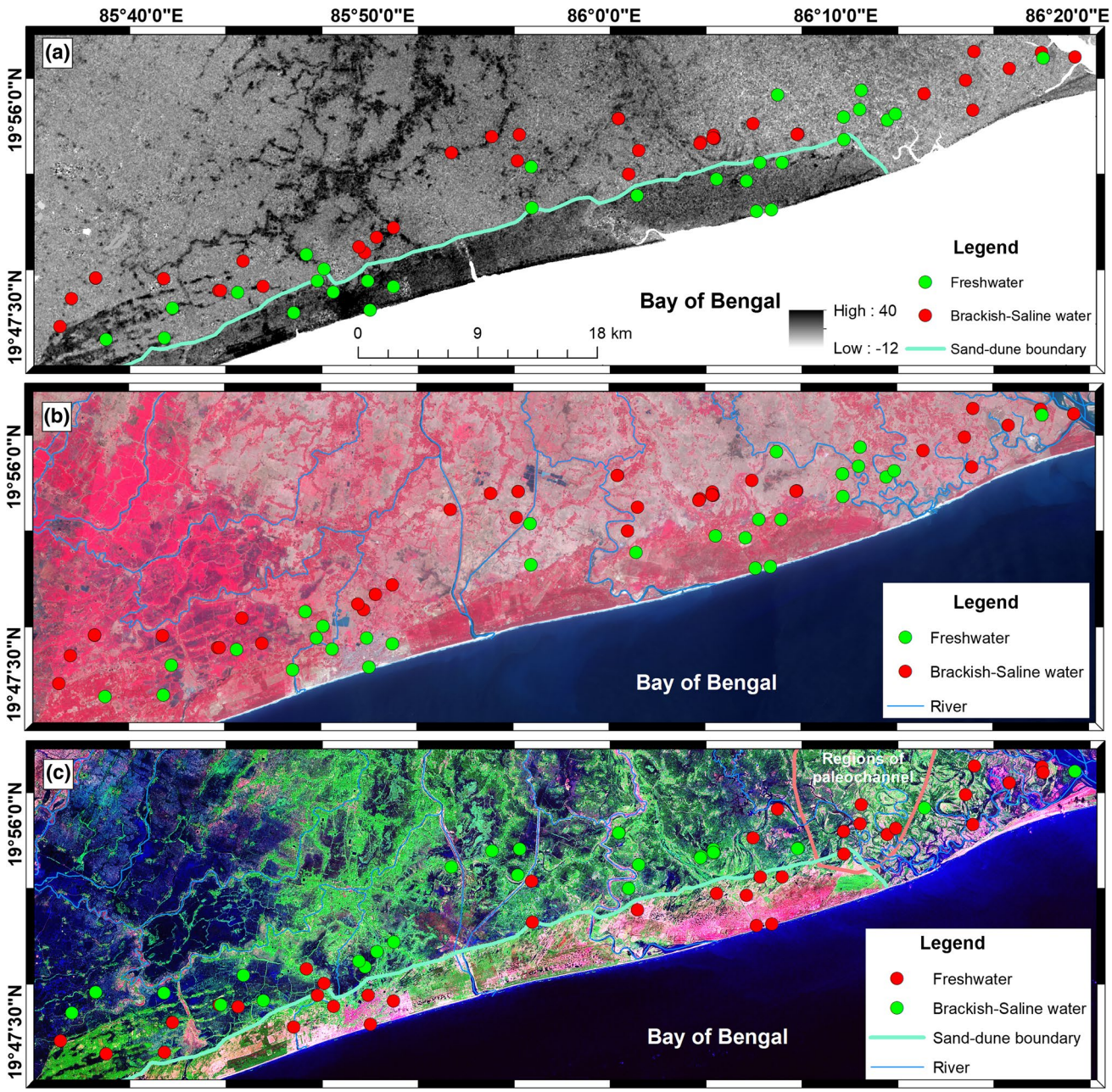

Fig. 8 Geographical distribution of fresh and brackish-saline groundwater on **a** digital elevation model, **b** false-color composite image, and **c** enhanced thematic mapper plus pan mosaic image

Acknowledgements The authors are thankful to the Ministry of Earth Sciences (MoES), Govt. of India for providing financial assistance through Bay of Bengal Coastal Observatory (RP-088) and IIT Bhubaneswar for extending the analytical facilities to carry out the work. The authors are also thankful to Open Topography Facility supported by US NSF (Award Numbers: 1833703, 1833643, and 1833632) and US Geological Survey for providing free access to remote sensing data. Mr. Ashish K. Tiwary, Mr. B. Sahoo, and Mr. Prabhas K. Mohanty are thanked for their valuable help in the fieldwork. The authors are very much thankful to Dr. M. Abbaspour (Editor-in-Chief) and the anonymous reviewers for their time and valuable suggestions to improve the manuscript.

Compliance with ethical standards

Ethical approval This article does not contain any studies with human participants or animals performed by any of the authors.

Appendix

See Table 3.

Table 3 Results of detailed analysis of individual groundwater samples

ID	pH	EC (µs/cm)	TDS (mg/l)	Alkalinity (mg/l)	Cl (mg/l)	SO_4 (mg/l)	Na (mg/l)	K (mg/l)	Ca (mg/l)	Mg (mg/l)
1	6.8	19,440	12,442	525.0	5753	575	3921	139	154	398
2	6.6	311.1	199.1	57.37	33.54	12.3	24.70	15.6	13.5	4.2
3	6.4	1976	1265	173.4	291.0	131	163.2	162	48.1	36.0
4	6.6	2728	1746	169.9	595.1	225	401.6	54.9	69.6	63.6
5	7.3	1680	1075	211.8	317.9	47.4	341.1	15.6	11.0	11.1
6	6.6	2033	1301	159.4	459.6	75.5	297.6	5.71	67.1	42.7
7	6.9	2544	1628	182.7	642.2	54.7	415.2	22.7	31.5	60.2
8	7.2	602.5	385.6	181.3	67.0	1.10	63.44	14.2	21.9	15.7
9	6.2	171.9	110	63.99	17.20	4.19	11.37	1.07	10.9	4.84
10	6.8	392.5	251.2	42.29	58.10	13.1	27.12	1.86	19.7	9.13
11	6.5	541.6	346.6	80.16	92.56	33.0	55.39	4.88	25.2	13.9
12	6.9	1424	911.4	121.1	331.9	36.3	156.5	16.2	48.4	44.7
13	6.6	1109	709.8	166.7	163.5	74.0	92.19	66.1	39.8	24.8
14	7.5	4519	2892	487.5	1099	2.75	891.3	25.2	28.5	43.0
15	7.7	197.2	126.2	76.84	22.89	0.40	10.67	4.89	20.0	5.11
16	7.9	1488	952.3	345.2	225.8	0.37	292.2	13.0	11.2	13.6
17	7.3	1842	1179	423.4	318.1	0.11	348.1	19.1	17.2	20.2
18	7.1	329.5	210.9	114.6	52.58	0.08	21.20	4.73	29.2	7.85
19	6.4	619.2	396.3	51.25	86.42	24.8	47.90	14.2	26.5	9.43
20	7.3	249.9	159.9	77.11	15.48	1.82	9.409	1.26	14.7	8.05
21	6.8	467.2	299	79.82	49.71	13.5	18.09	1.74	47.6	4.58
22	6.9	237.2	151.8	65.62	14.53	0.34	7.641	1.06	17.4	5.87
23	7.1	5433	3477	581.8	1244	5.36	746.5	160	155	131
24	7.6	3421	2189	442.6	744.9	0.08	669.5	17.9	29.8	30.5
25	7.2	4995	3197	501.0	1125	0.20	965.7	30.7	33.9	47.5
26	7.2	4372	2798	481.1	934.3	0.20	834.5	25.0	40.4	38.4
27	6.8	94.12	60.24	26.26	6.128	0.96	6.330	2.32	3.18	2.46
28	6.6	6242	3995	316.5	1583	96.2	1064	106	132	89.2
29	7.3	5387	3448	703.0	1181	0.33	1054	29.2	27.4	75.3
30	6.7	4013	2568	196.7	1067	116	683.7	8.44	107	46.6
31	6.7	4231	2708	170.0	1087	182	424.4	72.2	232	143
32	7.3	246.8	158	85.86	16.68	2.11	36.25	9.97	1.73	3.96
33	7.8	4288	2744	305.8	943.5	150	842.6	25.1	33.6	30.8
34	6.8	509.7	326.2	85.27	81.17	12.9	50.85	14.2	16.7	10.4
35	7.4	9635	6166	120.8	3065	181	1342	45.2	369	268
36	7.8	3715	2378	276.0	896.6	81.7	611.3	18.3	95.0	68.9
37	6.8	3094	1980	392.6	700.0	41.5	421.0	23.4	144	67.9
38	7.2	532.2	340.6	145.1	50.08	28.4	71.32	16.2	2.04	9.74
39	7.2	4287	2744	331.6	1022	209	708.1	35.5	86.0	92.9
40	6.8	3116	1994	259.7	451.1	498	504.3	35.5	83.5	75.1
41	6.9	5576	3569	160.1	1249	588	610.4	29.7	297	130
42	7.1	1075	688	213.7	160.6	23.7	110.2	25.4	34.9	35.1
43	7.4	1186	759	296.6	123.3	53.3	56.80	17.4	93.8	41.6
44	6.8	543.6	347.9	111.0	89.42	9.78	100.1	7.14	0.34	1.06
45	6.9	1227	785.3	162.6	203.0	58.7	151.2	17.1	16.5	23.2
46	7.1	665.1	425.7	157.8	76.29	30.2	75.82	17.5	10.3	18.8
47	8.0	1147	734.1	335.4	139.9	16.9	185.8	8.98	12.8	10.2
48	8.0	445.6	285.2	197.1	12.40	0.44	31.79	12.0	15.4	20.9
49	7.6	3188	2040	356.0	585.9	137	557.2	18.6	42.1	54.3
50	7.7	4629	2963	240.0	1259	47.1	693.2	32.0	64.7	35.2

Table 3 (continued)

ID	pH	EC (µs/cm)	TDS (mg/l)	Alkalinity (mg/l)	Cl (mg/l)	SO_4 (mg/l)	Na (mg/l)	K (mg/l)	Ca (mg/l)	Mg (mg/l)
51	8.2	974.7	623.8	380.7	56.91	12.9	204.2	8.80	11.8	8.32
52	6.9	19,980	12,787	97.22	6690	1203	2865	56.0	742	523
53	7.8	2257	1444	344.3	409.6	95.5	323.8	12.4	30.1	32.3
54	5.2	684.3	438	6.862	154.4	29.2	50.24	20.3	17.3	20.7
55	6.3	834.3	534	52.26	177.4	48.6	87.60	48.3	11.4	20.0
56	7.6	3237	2072	218.8	826.9	95.1	569.2	23.8	38.1	48.2
57	6.2	604.6	386.9	69.41	112.0	29.2	77.58	5.16	12.2	7.99
58	6.9	11,460	7334	312.8	3348	462	1645	128	380	302
59	7.4	4202	2689	235.4	1153	77.3	582.5	19.7	90.4	39.8
60	7.6	2787	1784	278.5	660.6	34.8	397.6	15.4	42.0	17.6
61	7.0	5450	3488	299.1	1450	218	748.8	85.7	254	137
62	7.0	1250	800	110.9	290.6	12.6	143.4	9.21	40.2	38.5
63	7.1	4168	2668	492.3	921.8	83.6	662.4	148	67.6	62.5
64	7.0	5517	3531	540.1	1297	0.36	827.7	95.4	170	112
65	6.9	4366	2794	438.5	1010	0.39	544.5	104	152	117
66	7.3	4452	2849	269.7	1084	107	795.6	17.3	93.3	53.7
67	6.2	21,180	13,555	95.42	7139	1433	2961	113	1069	797
68	6.9	5248	3359	239.3	1304	241	718.9	32.5	163	143

References

Abdalla F (2016) Ionic ratios as tracers to assess seawater intrusion and to identify salinity sources in Jazan coastal aquifer, Saudi Arabia. Arab J Geosci 9:1–12. https://doi.org/10.1007/s12517-015-2065-3

Abd-Elhamid H, Abdelaty I, Sherif M (2019) Evaluation of potential impact of Grand Ethiopian Renaissance Dam on seawater intrusion in the Nile Delta aquifer. Int J Environ Sci Technol 16:2321–2332. https://doi.org/10.1007/s13762-018-1851-3

Afrasinei GM, Melis MT, Arras C et al (2018) Spatiotemporal and spectral analysis of sand encroachment dynamics in southern Tunisia. Eur J Remote Sens 51:352–374. https://doi.org/10.1080/22797254.2018.1439343

Appelo C, Postma D (2005) Geochemistry, groundwater and pollution, 2nd edn. A A Balkema, Amsterdam

Aris AZ, Abdullah MH, Ahmed A, Woong KK (2007) Controlling factors of groundwater hydrochemistry in a small island's aquifer. Int J Environ Sci Technol 4:441–450. https://doi.org/10.1007/BF03325979

Barlow PM, Reichard EG (2010) Saltwater intrusion in coastal regions of North America. Hydrogeol J 18:247–260. https://doi.org/10.1007/s10040-009-0514-3

Batayneh AT, Al-Taani AA (2016) Integrated resistivity and water chemistry for evaluation of groundwater quality of the Gulf of Aqaba coastal area in Saudi Arabia. Geosci J 20:403–413. https://doi.org/10.1007/s12303-015-0053-y

Cary L, Petelet-Giraud E, Bertrand G et al (2015) Origins and processes of groundwater salinization in the urban coastal aquifers of Recife (Pernambuco, Brazil): a multi-isotope approach. Sci Total Environ 530–531:411–429. https://doi.org/10.1016/j.scitotenv.2015.05.015

Census of India (2011) CensusInfo India. http://www.dataforall.org/dashboard/censusinfoindia_pca/. Accessed 8 Aug 2016

Central Ground Water Board (2013) Groundwater information booklet, Puri District, Orissa. Ministry of Water Resources, Govt. of India, South Eastern Region, Bhubaneswar

Central Ground Water Board (2014) Report on status of ground water quality in coastal aquifers of India. Ministry of Water Resources, Govt. of India, Faridabad

Central Water Commission (2017) Problems of salination of land in coastal areas of India and suitable protection measures. Ministry of Water Resources, River Development & Ganga Rejuvenation, Govt. of India, New Delhi

Daliakopoulos IN, Tsanis IK, Koutroulis A et al (2016) The threat of soil salinity: a European scale review. Sci Total Environ 573:727–739. https://doi.org/10.1016/j.scitotenv.2016.08.177

Deverel SJ, Goldberg S, Fujii R (2011) Chemistry of trace elements in soils and groundwater. Agricultural salinity assessment and management, 2nd edn. American Society of Civil Engineers, Reston, pp 89–137

Dhakate R, Sankaran S, Kumar VS et al (2016) Demarcating saline water intrusion pathways using remote sensing, GIS and geophysical techniques in structurally controlled coastal aquifers in Southern India. Environ Earth Sci 75:363. https://doi.org/10.1007/s12665-015-4940-3

Freeze RA, Cherry JA (1979) Groundwater. Prentice-Hall Inc, Englewood Cliffs

Ghasemlounia R, Sedaghat Herfeh N (2017) Study on groundwater quality using geographic information system (GIS), case study: Ardabil, Iran. Civ Eng J 3:779–793. https://doi.org/10.21859/cej-030914

Giménez-Forcada E (2010) Dynamic of sea water interface using hydrochemical facies evolution diagram. Ground Water 48:212–216. https://doi.org/10.1111/j.1745-6584.2009.00649.x

Giménez-Forcada E (2019) Use of the hydrochemical facies diagram (HFE-D) for the evaluation of salinization by seawater intrusion in the coastal Oropesa Plain: comparative analysis with the coastal Vinaroz Plain, Spain. HydroResearch 2:76–84. https://doi.org/10.1016/j.hydres.2019.11.007

Gopalakrishnan T, Hasan MK, Haque ATMS et al (2019) Sustainability of coastal agriculture under climate change. Sustainability 11:7200. https://doi.org/10.3390/su11247200

Herbert ER, Boon P, Burgin AJ et al (2015) A global perspective on wetland salinization: ecological consequences of a growing threat to freshwater wetlands. Ecosphere 6:206. https://doi.org/10.1890/ES14-00534.1

Hoque MA, Scheelbeek PFD, Vineis P et al (2016) Drinking water vulnerability to climate change and alternatives for adaptation in coastal South and South East Asia. Clim Change 136:247–263. https://doi.org/10.1007/s10584-016-1617-1

Hussain MS, Javadi AA, Sherif MM (2015) Three dimensional simulation of seawater intrusion in a regional coastal aquifer in UAE. Procedia Eng 119:1153–1160. https://doi.org/10.1016/j.proeng.2015.08.965

Kanagaraj G, Elango L, Sridhar SGD, Gowrisankar G (2018) Hydrogeochemical processes and influence of seawater intrusion in coastal aquifers south of Chennai, Tamil Nadu, India. Environ Sci Pollut Res 25:8989–9011. https://doi.org/10.1007/s11356-017-0910-5

Kantamaneni K, Du X, Aher S, Singh RM (2017) Building blocks: a quantitative approach for evaluating coastal vulnerability. Water 9:905. https://doi.org/10.3390/w9120905

Lloyd JW, Heathcote JA (1985) Natural inorganic hydrochemistry in relation to groundwater: an introduction. Clarendon Press, Oxford

Manivannan V, Elango L (2019) Seawater intrusion and submarine groundwater discharge along the Indian coast. Environ Sci Pollut Res 26:31592–31608. https://doi.org/10.1007/s11356-019-06103-z

Michael HA, Russoniello CJ, Byron LA (2013) Global assessment of vulnerability to sea-level rise in topography-limited and recharge-limited coastal groundwater systems. Water Resour Res 49:2228–2240. https://doi.org/10.1002/wrcr.20213

Mirzavand M, Ghasemieh H, Sadatinejad SJ, Bagheri R (2020) An overview on source, mechanism and investigation approaches in groundwater salinization studies. Int J Environ Sci Technol. https://doi.org/10.1007/s13762-020-02647-7

MoEF & CC (2016) Coastal districts of India. In: Centre for coastal zone management and coastal shelter belt. http://iomenvis.nic.in/index2.aspx?slid=3680&sublinkid=259&langid=1&mid=1. Accessed 21 Jan 2017

Mohanty AK, Rao VVSG (2019) Hydrogeochemical, seawater intrusion and oxygen isotope studies on a coastal region in the Puri District of Odisha, India. CATENA 172:558–571. https://doi.org/10.1016/j.catena.2018.09.010

Mohapatra PK, Vijay R, Pujari PR et al (2011) Determination of processes affecting groundwater quality in the coastal aquifer beneath Puri city, India: a multivariate statistical approach. Water Sci Technol 64(4):809–817. https://doi.org/10.2166/wst.2011.605

Mondal NC, Singh VP, Singh VS, Saxena VK (2010) Determining the interaction between groundwater and saline water through groundwater major ions chemistry. J Hydrol 388:100–111. https://doi.org/10.1016/J.JHYDROL.2010.04.032

Nair IS, Brindha K, Elango L (2016) Identification of salinization by bromide and fluoride concentration in coastal aquifers near Chennai, southern India. Water Sci 30:41–50. https://doi.org/10.1016/j.wsj.2016.07.001

Najib S, Fadili A, Mehdi K et al (2017) Contribution of hydrochemical and geoelectrical approaches to investigate salinization process and seawater intrusion in the coastal aquifers of Chaouia, Morocco. J Contam Hydrol 198:24–36. https://doi.org/10.1016/j.jconhyd.2017.01.003

Nandini CV, Sanjeevi S, Bhaskar AS (2013) An integrated approach to map certain palaeochannels of South India using remote sensing, geophysics, and sedimentological techniques. Int J Remote Sens 34:6507–6528. https://doi.org/10.1080/01431161.2013.803629

Ngo MT, Lee JM, Lee HA, Woo NC (2015) The sustainability risk of Ho Chi Minh City, Vietnam, due to saltwater intrusion. Geosci J 19:547–560. https://doi.org/10.1007/s12303-014-0052-4

Nielsen DL, Brock MA, Rees GN, Baldwin DS (2003) Effects of increasing salinity on freshwater ecosystems in Australia. Aust J Bot 51:655–665. https://doi.org/10.1071/BT02115

Oram B (2011) The pH of water. In: Water research center information on water testing/water treatment. http://www.water-research.net/index.php/ph. Accessed 11 Jan 2017

Owen R, Dahlin T (2010) Inherited drainage—paleochannels and preferential groundwater flow. Hydrogeol J 18:893–903. https://doi.org/10.1007/s10040-010-0588-y

Park SC, Yun ST, Chae GT et al (2005) Regional hydrochemical study on salinization of coastal aquifers, western coastal area of South Korea. J Hydrol 313:182–194. https://doi.org/10.1016/j.jhydrol.2005.03.001

Patra JP, Mishra A, Singh R, Raghuwanshi NS (2012) Detecting rainfall trends in twentieth century (1871–2006) over Orissa State, India. Clim Change 111:801–817. https://doi.org/10.1007/s10584-011-0215-5

Pink RM (2018) Africa: Kenya, South Africa, Botswana. The climate change crisis. Springer, Cham, pp 125–162

Prasanth SVS, Magesh NS, Jitheshlal KV et al (2012) Evaluation of groundwater quality and its suitability for drinking and agricultural use in the coastal stretch of Alappuzha District, Kerala, India. Appl Water Sci 2:165–175. https://doi.org/10.1007/s13201-012-0042-5

Prusty P, Farooq SH, Zimik HV, Barik SS (2018) Assessment of the factors controlling groundwater quality in a coastal aquifer adjacent to the Bay of Bengal, India. Environ Earth Sci 77:762. https://doi.org/10.1007/s12665-018-7943-z

Putra DBE, Yuskar Y, Kausarian H et al (2019) Saltwater intrusion zone mapping on shallow groundwater aquifer in Selat Baru, Bengkalis Island, Indonesia. J Geosci Eng Environ Technol 4:16. https://doi.org/10.25299/jgeet.2019.4.1.2672

Rakib MA, Sasaki J, Matsuda H et al (2020) Groundwater salinization and associated co-contamination risk increase severe drinking water vulnerabilities in the southwestern coast of Bangladesh. Chemosphere 246:125646. https://doi.org/10.1016/j.chemosphere.2019.125646

Re V, Misstear B (2017) Education and capacity development for groundwater resources management. In: Villholth KG, Lopez-Gunn E, Conti K, Garrido A, Van Der Gun J (eds) Advances in groundwater governance. CRC Press, Boca Raton, pp 215–230

Rice EW, Baird RB, Eaton AD, Clesceri LS (eds) (2012) Standard methods for the examination of water and wastewater, 22nd edn. American Public Health Association, Washington, DC

Saintilan N, Rogers K, Kelleway JJ et al (2018) Climate change impacts on the coastal wetlands of Australia. Wetlands. https://doi.org/10.1007/s13157-018-1016-7

Sajil Kumar PJ, Elango L, James EJ (2014) Assessment of hydrochemistry and groundwater quality in the coastal area of South Chennai, India. Arab J Geosci 7:2641–2653. https://doi.org/10.1007/s12517-013-0940-3

Scheidleger A, Grath J, Lindinger H (2004) Saltwater intrusion due to groundwater over-exploitation EEA inventory throughout Europe. In: 18th salt water intrusion meeting, Cartagena, Spain

Schneider JC, Kruse SE (2003) A comparison of controls on freshwater lens morphology of small carbonate and siliciclastic islands: examples from barrier islands in Florida, USA. J Hydrol 284:253–269. https://doi.org/10.1016/j.jhydrol.2003.08.002

Shi L, Jimmy J (2014) Seawater intrusion and coastal aquifer management in China: a review. Environ Earth Sci 72:2811–2819. https://doi.org/10.1007/s12665-014-3186-9

Sinclair AJ (1974) Selection of threshold values in geochemical data using probability graphs. J Geochem Explor 3:129–149. https://doi.org/10.1016/0375-6742(74)90030-2

Sola F, Vallejos A, Moreno L et al (2013) Identification of hydrogeochemical process linked to marine intrusion induced by pumping

of a semiconfined mediterranean coastal aquifer. Int J Environ Sci Technol 10:63–76. https://doi.org/10.1007/s13762-012-0087-x

Solangi GS, Siyal AA, Siyal P (2019) Analysis of Indus Delta groundwater and surface water suitability for domestic and irrigation purposes. Civ Eng J 5:1599–1608. https://doi.org/10.28991/cej-2019-03091356

Sun M, Wong D, Kronenfeld B (2017) A heuristic multi-criteria classification approach incorporating data quality information for choropleth mapping. Cartogr Geogr Inf Sci 44:246–258. https://doi.org/10.1080/15230406.2016.1145072

Vijay R, Sharma A, Ramya SS, Gupta A (2011) Fluctuation of groundwater in an urban coastal city of India: a GIS-based approach. Hydrol Process 25:1479–1485. https://doi.org/10.1002/hyp.7914

Viso R, McCoy C, Gayes P, Quafisi D (2010) Geological controls on submarine groundwater discharge in Long Bay, South Carolina (USA). Cont Shelf Res 30:335–341. https://doi.org/10.1016/j.csr.2009.11.014

Yamanaka M, Bottrell SH, Wu J et al (2014) Chlorine stable isotope evidence for salinization processes of confined groundwater in southwestern Nobi Plain aquifer system, central Japan. J Hydrol 519:295–306. https://doi.org/10.1016/j.jhydrol.2014.07.022

Zhang L (2019) Big data, knowledge mapping for sustainable development: a water quality index case study. Emerg Sci J 3:249–254. https://doi.org/10.28991/esj-2019-01187